1998-03-01

Communications antenna for a micro RPV

Suksong, Narongdech

Monterey, California. Naval Postgraduate School

http://hdl.handle.net/10945/8103

NAVAL POSTGRADUATE SCHOOL
Monterey, California

THESIS

COMMUNICATIONS ANTENNA
FOR
A MICRO RPV

by

Narongdech Suksong

March 1998

Thesis Advisor: David C. Jenn
Second Reader: Supachai Sirayanone

REPORT DOCUMENTATION PAGE

Form Approved
OMB No. 0704-0188

Public reporting burden for this collection of information is estimated to average 1 hour per response, including the time for reviewing instruction, searching existing data sources, gathering and maintaining the data needed, and completing and reviewing the collection of information. Send comments regarding this burden estimate or any other aspect of this collection of information, including suggestions for reducing this burden, to Washington headquarters Services, Directorate for Information Operations and Reports, 1215 Jefferson Davis Highway, Suite 1204, Arlington, VA 22202-4302, and to the Office of Management and Budget, Paperwork Reduction Project (0704-0188) Washington DC 20503.

1. AGENCY USE ONLY *(Leave blank)*	2. REPORT DATE March 1998	3. REPORT TYPE AND DATES COVERED Master's Thesis

4. TITLE AND SUBTITLE COMUNICATIONS ANTENNA FOR A MICRO RPV	5. FUNDING NUMBERS
6. AUTHOR(S) Suksong, Narongdech	

7. PERFORMING ORGANIZATION NAME(S) AND ADDRESS(ES) Naval Postgraduate School Monterey, CA 93943-5000	8. PERFORMING ORGANIZATION REPORT NUMBER

9. SPONSORING / MONITORING AGENCY NAME(S) AND ADDRESS(ES)	10. SPONSORING / MONITORING AGENCY REPORT NUMBER

11. SUPPLEMENTARY NOTES

The views expressed in this thesis are those of the author and do not reflect the official policy or position of the Department of Defense or the U.S. Government.

12a. DISTRIBUTION / AVAILABILITY STATEMENT Approved for public release; distribution is unlimited.	12b. DISTRIBUTION CODE

13. ABSTRACT *(maximum 200 words)*

The objective of this research was to design a compact lightweight communications antenna for a micro remotely piloted vehicle (MRPV). Based on a computer simulation of four potential antenna configurations it was found that a monopole on a cylindrical end cap provides the lowest voltage standing wave ratio (VSWR) and a nearly hemispherical radiation pattern. The data was generated at frequencies near 1 GHz using two methods of moment computational electromagnetic codes: PATCH and NEC-Win.

14. SUBJECT TERMS RPV, PATCH, NEC-Win, and antennas.			15. NUMBER OF PAGES 54
			16. PRICE CODE

17. SECURITY CLASSIFICATION OF REPORT Unclassified	18. SECURITY CLASSIFICATION OF THIS PAGE Unclassified	19. SECURITY CLASSIFI- CATION OF ABSTRACT Unclassified	20. LIMITATION OF ABSTRACT UL

NSN 7540-01-280-5500

Standard Form 298 (Rev. 2-89)

COMMUNICATIONS ANTENNA FOR A MICRO RPV

Narongdech Suksong
Second Lieutenant, Royal Thai Air Force
B.S.E.E., The Citadel, 1995

Submitted in partial fulfillment of the
requirements for the degree of

MASTER OF SCIENCE IN SYSTEMS ENGINEERING

from the

NAVAL POSTGRADUATE SCHOOL
March 1998

ABSTRACT

The objective of this research was to design a compact lightweight communications antenna for a micro remotely piloted vehicle (MRPV). Based on a computer simulation of four potential antenna configurations it was found that a monopole on a cylindrical end cap provides the lowest voltage standing wave ratio (VSWR) and a nearly hemispherical radiation pattern. The data was generated at frequencies near 1 GHz using two method of moments computational electromagnetic codes: **PATCH** and **NEC-Win**.

TABLE OF CONTENTS

ACKNOWLEDGEMENT

This thesis dedicated to Prof. David C. Jenn, Dr. Supachai Sirayanone, and Commander Michael T. McMaster for their help and support.

I. INTRODUCTION

A. BACKGROUND

The concept of a remotely piloted vehicle (RPV) has been around for many years [Ref. 1]. A RPV is designed to be operated by a pilot or controller who is outside of the vehicle. A common example of a RPV is a radio controlled model airplane with a sensor or detector. The sensor is used to determine the motion, orientation, and location of the airplane relative to the terrain. Usually the sensor is a video camera, but radar and infrared systems also can be used.

RPVs have many advantages over manned vehicles. The obvious one is that RPVs do not expose the pilot to dangerous situations. Because of this, RPVs have always been of interest to the military. Another advantage is that RPVs do not need pilot support systems; therefore, it is possible to reduce the size and weight of the vehicles. But there are some disadvantages as well. One is that the sensor information from the vehicle must be of high quality and communicated to the ground station in real time. The US Department of Defense (DOD) is currently conducting research on miniature flying RPVs for military and civilian applications. These so-called micro RPVs (MRPVs) have been the subject of research for the last couple of years [Ref. 2].

The power source for propulsion and the onboard systems has been the major limitation in reducing the size of RPVs [Ref. 2]. Current battery and fuel cell technology is not able to achieve the size, weight and duration goals simultaneously. Generally, the power output of these sources is proportional to volume. If the battery is a cube with sides of length l (volume = l^3), then halving the dimensions reduces the power by factor

of 1/8. New battery and fuel cell technologies such as lithium polymers are yielding higher power densities and can be built as multiple layers and shaped to conform to the body surface.

Other power sources such as gas powered engines have essentially the same problem: the smaller the vehicle, the lower the power output and the smaller the amount of fuel that can be carried. Because of these shortcomings, off-board power sources have been considered. One of these concepts is to use microwave wireless power transmission (WPT) to beam energy to the vehicle. Previous research [Ref. 1] has examined the issues involved in the design and operation of a microwave powered MRPV, and WPT has been demonstrated for a MRPV which is shown in Figure 1.1. The power for the MRPV will come from the carrier signal transmitted from ground stations; therefore, this microwave-powered version will be very small and operation limited to relatively short ranges.
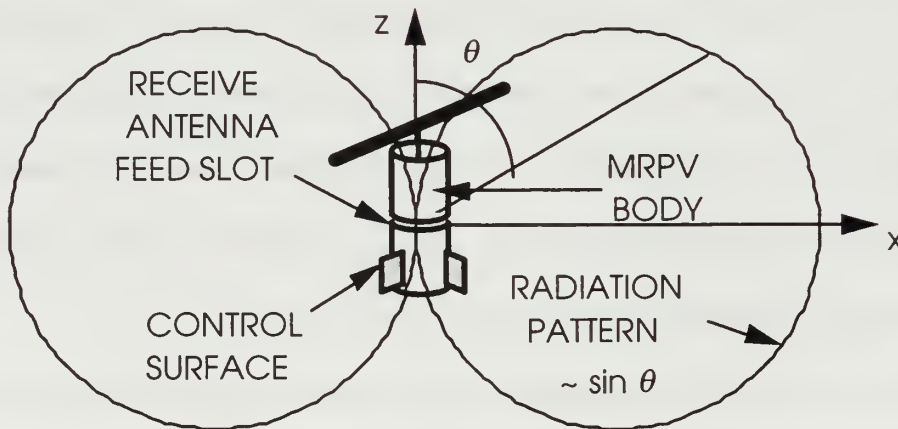

Figure 1.1 The microwave powered version of the RPV (after [Ref. 1]).

The aerodynamics of such a small vehicle is also the subject of much research because the straightforward approach of scaling does not give adequate results [Ref. 2].

2

The Defense Advanced Research Projects Agency (DARPA) has funded several contractors to demonstrate their approaches to aerodynamic, control, packaging and weight reduction. This involves near term (summer 1998) flight demonstrations. These MRPV models will be powered by conventional onboard energy sources, because the primary objectives are the demonstration of controlled flight and data gathering.

The demonstration models are required to send video data back to the pilot as well as receive command and control signals from the pilot. Therefore, the gas-powered version requires a transmitter and antenna on the vehicle to transmit the video data to the ground station. The most important requirement is that the antenna must be lightweight and have nearly isotropic coverage. Some candidate antennas include monopoles and loops. A short strip or wire hanging from the bottom of the vehicle as illustrated in Figure 1.2 (a monopole) is proposed.
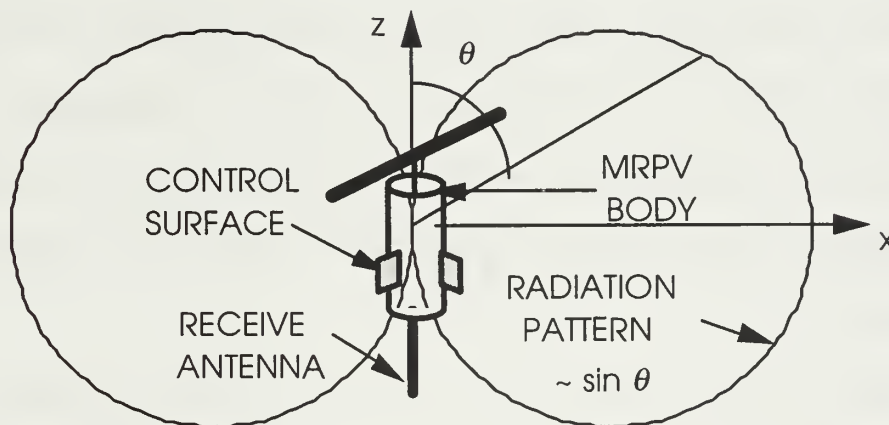

Figure 1.2 The conventional powered version of the RPV with a monopole antenna.

B.   APPROACH

All of the RPV systems are enclosed in the cylindrical body [Ref. 1]. They include the gas engine, transmitter, control electronics and the video camera. This research utilizes several electromagnetic simulation programs, such as **PATCH** and **NEC-Win**[†], for designing the antenna for the gas-engine version of the RPV. The microwave powered RPV uses a dipole type antenna, which is obtained by applying a metallic coating to the body. The dipole has a length of 4" and diameter of 1.5", which is the size of the RPV. Compared to the microwave-powered version, the antenna on the demonstration model does not have to be as efficient or handle as much power [Ref. 1]. Since weight must be minimized for the demonstration, the body must be constructed of graphite and metal must be avoided. The monopole antenna has nearly isotropic coverage and has the minimum weight of all the antenna configurations considered.

The proposed antenna design is primarily comprised of two parts: a disc (finite ground plane) and a small strip or wire. In addition, it is possible to add a thin conducting film to the body in order to match the input impedance, if necessary. The primary design criteria are a broad radiation pattern and an input impedance near 50 Ohms (an input Voltage Standing Wave Ratio (VSWR) of 2:1 or less). Although the antenna gain is not a major concern, the antenna losses should not be excessive (perhaps 2 dB at most).

Chapter II reviews some antenna theory and its important parameters such as directivity, gain, input impedance, and VSWR. Chapter III gives a brief description of the simulation tools, **PATCH** and **NEC-Win,** and their capabilities.   Chapter IV

[†] Throughout this thesis computer codes and file names are signified by boldface names.

addresses the design of the monopole and other candidate antenna configurations. Finally

Chapter V presents conclusions and recommendations for future research.

II. DIPOLE, MONOPOLE, AND LOOP ANTENNAS

A.   INTRODUCTION

An antenna can be simply described as a good conducting material that has been designed to have a shape and size such that it will radiate electromagnetic power in an efficient manner. In order to radiate efficiently, the minimum size of the antenna must be comparable to a half wavelength [Ref. 3]. One of the most common antennas is the half-wavelength dipole antenna, which consists of two conducting rods. Each rod is one-quarter wavelength long and is separated by a small gap. This gap is connected to a voltage source via a transmission line. In many applications it is possible to replace one arm of the dipole with a ground plane. This configuration is referred to as a monopole. In this chapter the performance parameters of antennas such as *radiation pattern*, *directivity*, *gain*, *radiation impedance*, and *voltage standing wave ratio* (VSWR) are defined [Refs. 3-6]. Also the characteristics of ideal dipoles, loops, and monopoles are discussed [Ref. 4].

B.   DESIGN PARAMETERS

1.   Radiation Pattern

The radiation pattern of the antenna is the relative distribution of radiated power as a function of direction in space [Ref. 3]. When plotted, it is a graphical representation of the received signal strength for a constant transmit power. It can be measured by moving a probe antenna around the test antenna at a constant distance (i.e., on the surface of a sphere). A typical monopole antenna power pattern is illustrated in Figure 2.1 as a

polar plot in linear units. In Figure 2.1, the excited end is at the center and the other end at $\theta = 0°$. The power pattern also can be shown in decibels (dB). An ideal short dipole is shown in Figure 2.2. The overall length of the dipole for the most effective operation is about $\frac{\lambda}{2}$ (λ = wavelength), although dipoles can be much shorter. An ideal quarter-wavelength monopole is shown in Figure 2.3. A small loop antenna, which is shown in Figure 2.4, is the magnetic dual of the electric dipole. For the dipole antenna and the monopole, there are no side lobes, and they are almost perfect isotropic radiators. *An isotropic radiator* or antenna is defined as a fictitious antenna that radiates uniformly in all directions and is commonly used as a reference. Another meaningful parameter is the *half-power beamwidth*, which is defined as the angular width between points at which the radiated power per unit area is one-half of the maximum.
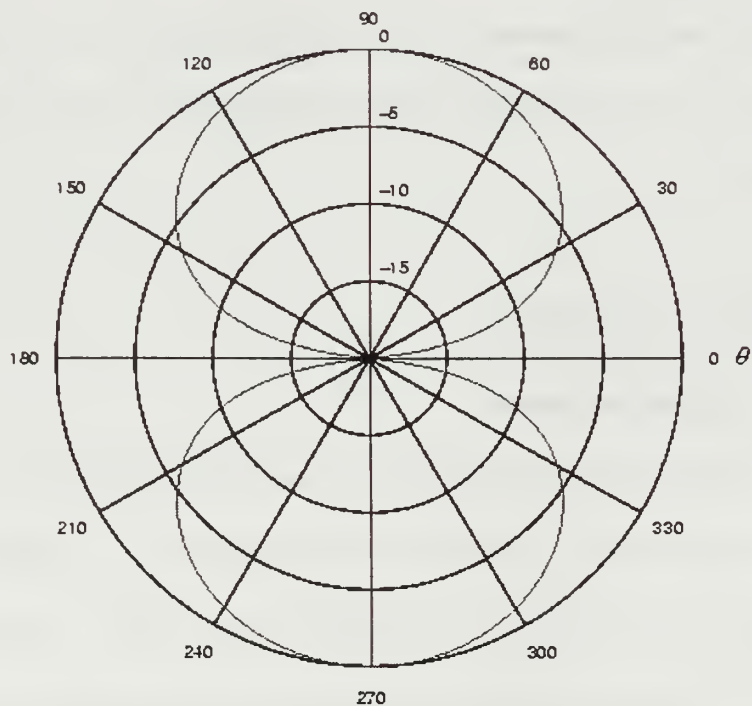

Figure 2.1 The dipole power pattern (θ in this figure is the same as in Figures 2.2 through 2.4).
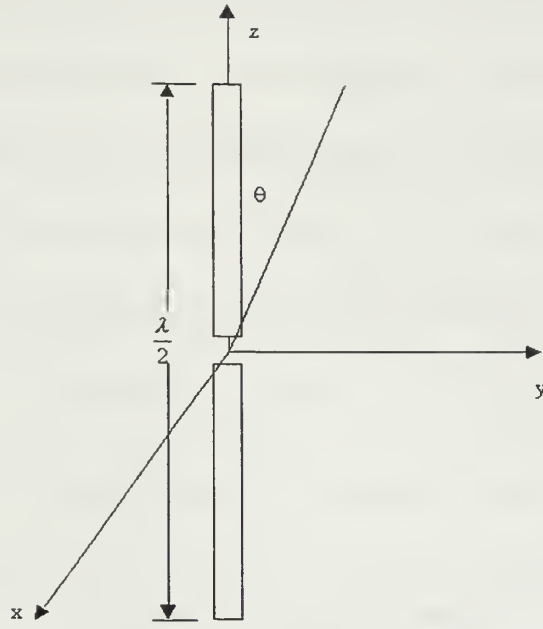
Figure 2.2 An ideal half wavelength dipole.
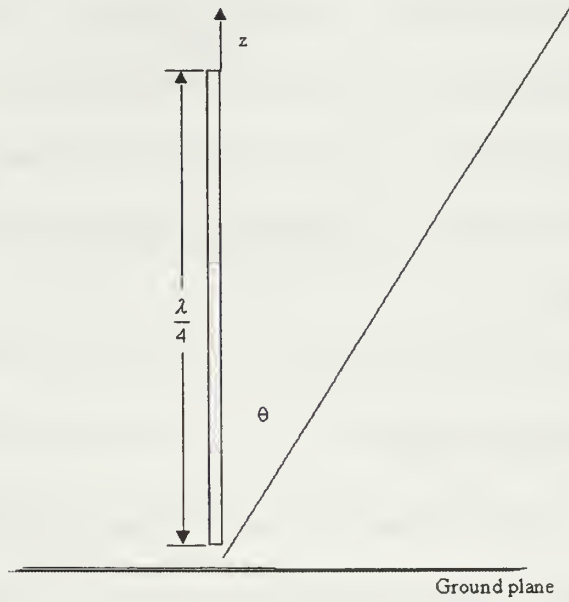
Figure 2.3 An ideal quarter-wavelength monopole.
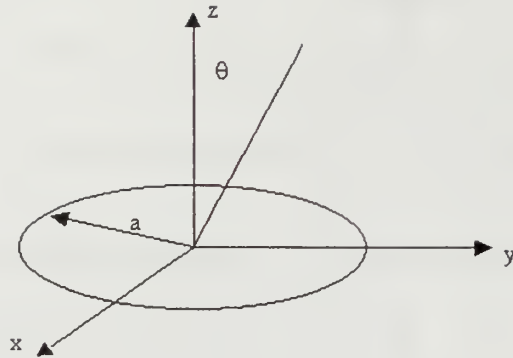
Figure 2.4 A small loop antenna.

The radiation pattern of a monopole on a perfect ground plane is the same as the dipole antenna in free space [Ref. 3]. From image theory, the current above a perfect ground plane is the same as that below the ground except opposite in direction. The voltage across the monopole gap is only half that of the dipole. The reason is that the gap width of the input terminals is half of the dipole. Therefore the monopole antenna with an infinite ground is equivalent to a dipole antenna of the same length as far as the radiation pattern is concerned [Ref. 3]. However, the monopole impedance is generally less than that of the dipole.

2.   Directivity and Gain

All antennas do not radiate uniformly in all directions [Ref. 4]. The variation of the intensity with direction in space is described by the *directivity* function

$$D(\theta,\phi) = \frac{dP_r/d\Omega}{P_r/4\pi} \tag{II-1}$$

where $dP_r/d\Omega$ is the intensity of radiation, which is expressed in terms of the power

radiated (P_r) per unit solid angle (Ω). θ is the angle that is measured from the z axis, and

ϕ is the angle is measure from the x axis (or x-z plane). Sometimes θ is called the *zenith*

angle, and ϕ is called the *azimuth* angle. The ratio $P_r/4\pi$ is the average power radiated

per unit solid angle. The directive gain also can be written as

$$D(\theta,\phi) = D|F(\theta,\phi)|^2 \tag{II-2}$$

where $|F(\theta,\phi)|^2$ is a function that has a maximum value of unity. Therefore, the

maximum of the directive gain is the directivity (simply denoted D). For the dipole the

total radiated power is defined as [Ref. 4]

$$P_r = \frac{II^*Z_0(dl)^2 k_0^2}{32\pi^2} \int_0^{2\pi}\int_0^{\pi} \sin^2\theta \sin\theta d\theta d\phi \tag{II-3}$$

or

$$P_r = \frac{II^*Z_0(dl)^2}{12\pi} \tag{II-4}$$

and

$$\frac{dP_r}{d\Omega} = \frac{II^*Z_0(dl)^2 k_0^2 \sin^2\theta}{32\pi^2} \tag{II-5}$$

where I is the current in the wire and "*" denotes a conjugate operation. Z_O is the

intrinsic impedance which equals $\sqrt{\mu_0/\varepsilon_0}$ ($= 120\pi$ Ohms), dl is the length of a short

dipole, and $k_0 = \omega\sqrt{\mu_0\varepsilon_0}$ is the free-space wave number. Where ω is the angular

frequency ($= 2\pi f$) [rad s^{-1}] μ_0 is the permeability of vacuum [H m^{-1}], and ε_0 is the

permittivity of vacuum [F m^{-1}].

Substituting Equation (II-4) and Equation (II-5) in Equation (II-1) gives

$$D(\theta,\phi) = 1.5\sin^2\theta. \tag{II-6}$$

From Equation (II-6), the maximum directivity D is 1.5 and occurs at the angle $\theta = \pi/2$

[Ref. 4]. Using the dipole antenna as an example, it produces 1.5 times the power density

in the $\theta = \pi/2$ direction than an isotropic radiator.

The *gain* of an antenna is defined similar to the directivity, except that the total

input power to the antenna rather than the total radiated power is used as the reference.

Therefore the gain of an antenna may be defined as follows [Ref. 4]:

$$G(\theta,\phi) = \frac{dP_r/d\Omega}{P_{in}/4\pi} \tag{II-7}$$

or

$$G(\theta,\phi) = 4\pi\frac{dP_r/d\Omega}{P_{in}} = \eta D(\theta,\phi) \tag{II-8}$$

and

$$P_r = \eta P_{in} \tag{II-9}$$

where P_{in} is the input power, and η is the *radiation efficiency*.

Since the monopole voltage across the terminals is half that of the dipole, the total

power of the monopole is also half that of the dipole [Ref. 3]. Equivalently, the beam

solid angle of a monopole above a perfect ground plane is one-half that of the dipole in

free space. Therefore, the monopole directivity can be defined as

$$D_{mono} = \frac{4\pi}{\Omega_{A,mono}} = \frac{4\pi}{\frac{1}{2}\Omega_{A,dipole}} \tag{II-10}$$

$$D_{mono} = 2D_{dipole} \tag{II-11}$$

3. Antenna Impedance

The input impedance of an antenna is the impedance presented by the antenna at its terminals [Ref. 2-6]. The input impedance (Z_{in}) is composed of real (R_{in}) and imaginary (jX_{in}) parts. The input resistance (R_{in}) can be found from the relation $P_r = \frac{1}{2}|I|^2 R_{in}$ and Equation (II-4). Thus the input resistance of the dipole antenna is defined as

$$R_{in,dipole} = \frac{Z_0(k_0 dl)^2}{6\pi} = 80\pi^2 \left(\frac{dl}{\lambda}\right)^2. \qquad \text{(II-12)}$$

For a monopole antenna, the current is the same as the dipole, but the voltage across the terminals is half of the dipole. Therefore the input resistance will be half of the dipole

$$R_{in,mono} = 160\pi^2 \left(\frac{h}{\lambda}\right)^2 \qquad \text{(II-13)}$$

where h is the length of the monopole antenna $(h = 0.5dl)$. Ideally the input impedance should be a constant resistance equal to the radiation resistance in order to have maximum power transfer [Ref. 5].

4. Voltage Standing Wave Ratio

Let the antenna impedance be $Z_L (= Z_{in})$ and the transmission line impedance Z_C, as shown in Figure 2.5. The load reflection coefficient Γ_L is given by [Ref. 4]

$$\Gamma_L = \frac{Z_L - Z_C}{Z_L + Z_C} \qquad \text{(II-14)}$$

where Z_C is the characteristic impedance of the transmission line. The voltage standing wave ratio (VSWR) is defined as the ratio of the maximum voltage to minimum voltage on the line:

$$\text{VSWR} = \frac{V_{max}}{V_{min}} = \frac{|V^+| + |V^-|}{|V^+| - |V^-|}. \tag{II-15}$$

It also can be written as a function of load reflection coefficient Γ_L

$$\text{VSWR} = \frac{1 + |\Gamma_L|}{1 - |\Gamma_L|}. \tag{II-16}$$

For most applications, the impedance match is usually considered acceptable if the VSWR is less than 1.5 [Ref. 5]. Given that Z_C is known and fixed, the VSWR specification sets the range of acceptable values for Z_{in}.
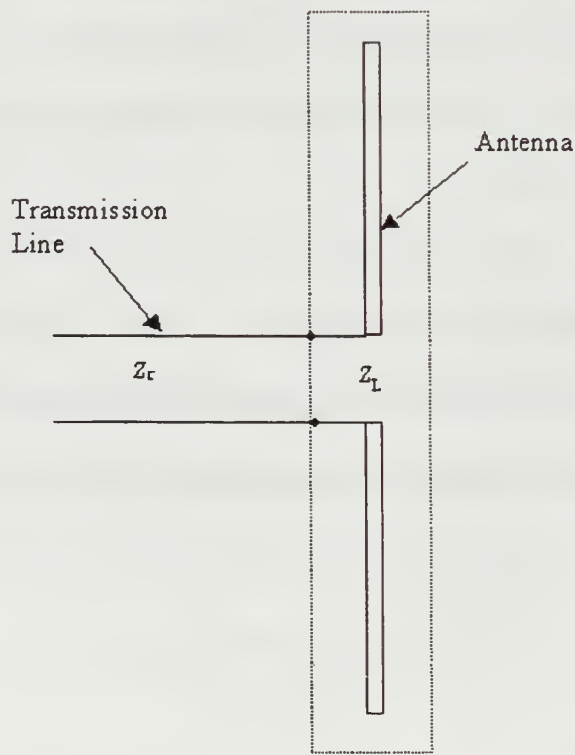

Figure 2.5 A half-wave dipole antenna coupled to a transmission line (after [Ref. 4]).

III. COMPUTER CODE DESCRIPTIONS

A. INTRODUCTION

This chapter briefly describes two of the most commonly used electromagnetic simulation codes [Refs. 7-8]. They are **PATCH** and **NEC-Win**. **PATCH** is a FORTRAN computer code that provides the ability to compute radar cross section (RCS) and radiation patterns using the integration of surface currents. **NEC-Win** is a software package that helps antenna designers quickly and effectively design and analyze antennas using wires to represent the physical antenna surfaces.

There are advantages and disadvantages to both **NEC-Win** and **PATCH**. **PATCH** can handle various types of materials that could be used to build the antenna, but **NEC-Win** structures are restricted to perfect electric conductors. The **PATCH** model is created by discretizing the solid object into triangular facets. Therefore, it is a more accurate representation for the antenna. **NEC-Win** uses thin wires to create the antenna model. When the actual antenna is built, some adjustment of the computed design parameters may be necessary. **NEC-Win** provides many options for output such as pattern plot, VSWR vs. frequency, gain, impedance, and so on. Users just click a tool button to specify which output options are desired. In this research both simulation programs are used. First **NEC-Win** was used to perform tradeoffs for all of the antenna parameters because it yields solutions faster than **PATCH**. Finally, **PATCH** was used to verify the design and "fine-tune" the parameters obtained from **NEC-Win**.

The calculations performed by **NEC-Win** and **PATCH** are based on a method of moments (MM) solution of the E-field integral equation (EFIE) which can be found in

more detail in [Ref. 3-6]. The method of moments reduces the EFIE to a system of simultaneous linear algebraic equations. Using standard matrix methods can solve for the unknown current. Once the current is known, it is a fairly straightforward procedure to determine the radiation pattern and impedance [Ref. 3].

The fundamental difference between **PATCH** and **NEC-Win** is that **PATCH** computes the surface currents ($\bar{J}_s$) on triangular facets, whereas **NEC-Win** computes the currents (I) that flow on a wire mesh that approximates the surface [Ref. 7-8]. The wire mesh approximation is accurate if the mesh dimensions are small relative to the wavelength. This approach allows some reduction in the computational load because the thin wire approximation can be used. For thin wires, only the component of current along the wire axis is significant. The component of current directed around the circumference of the wire is negligible.

It can be shown mathematically that the method employed by **PATCH** is rigorous [Ref. 6]. If the sizes of the triangular facets are reduced then **PATCH**'s result converges to the correct result (neglecting numerical and roundoff errors). On the other hand, the approach used by **NEC-Win** does not necessarily converge to the correct result if the wire mesh is reduced indefinitely.

In **PATCH,** the surface current density $\bar{J}_s$ is approximated by the sum of N terms where each term is the product of a known basis function $\bar{f}_n(\bar{r})$ and an unknown complex coefficient I_n [Ref. 3-4,6]

$$\bar{J}_S(\bar{r}) \approx \sum_{n=1}^{N} I_n \bar{f}_n(\bar{r}) \tag{III-1}$$

16

The basis function $\bar{f}_n(\bar{r})$ describes the current crossing edge n. For **PATCH,** the number of the triangle edges that are used to represent the given geometrical antenna determines the size of the matrix equation that must be solved for N unknowns. The area between edges that form the triangle facet is solid material. Therefore the current flows not only on the surface of the object, but also along the edges of the object. When the triangles become smaller, the number of unknowns increases. The rule of thumb for a converged solution is that the triangle edge lengths should not exceed 0.1 wavelength [Ref. 7].

For **NEC-Win,** the number of segments in the wire mesh determines the matrix size. Some additional unknowns are required to model the current behavior at junctions, because Kirchhoff's current law must be satisfied [Ref. 8]. Users tell **NEC-Win** how many segments comprise each mesh wire. As in the case of **PATCH**, the general rule of thumb is that each segment should not exceed 0.1 wavelength.

B.   PATCH

In this section we explain briefly the sequence of steps involved in building the facet model, running **PATCH**, and displaying the results [Ref. 7]. The following steps are illustrated in Figure 3.1.

1.   Create and mesh the antenna geometry model.

There are two ways to create the antenna model. It can be created by using CAD applications (such as Auto-CAD or ACAD) or by using the code **buildn5.x**[†]. This file will be used in steps 2 and 3.

[†] **buildn5.x** is a geometry generator with limited capability which is distributed along with **PATCH.**
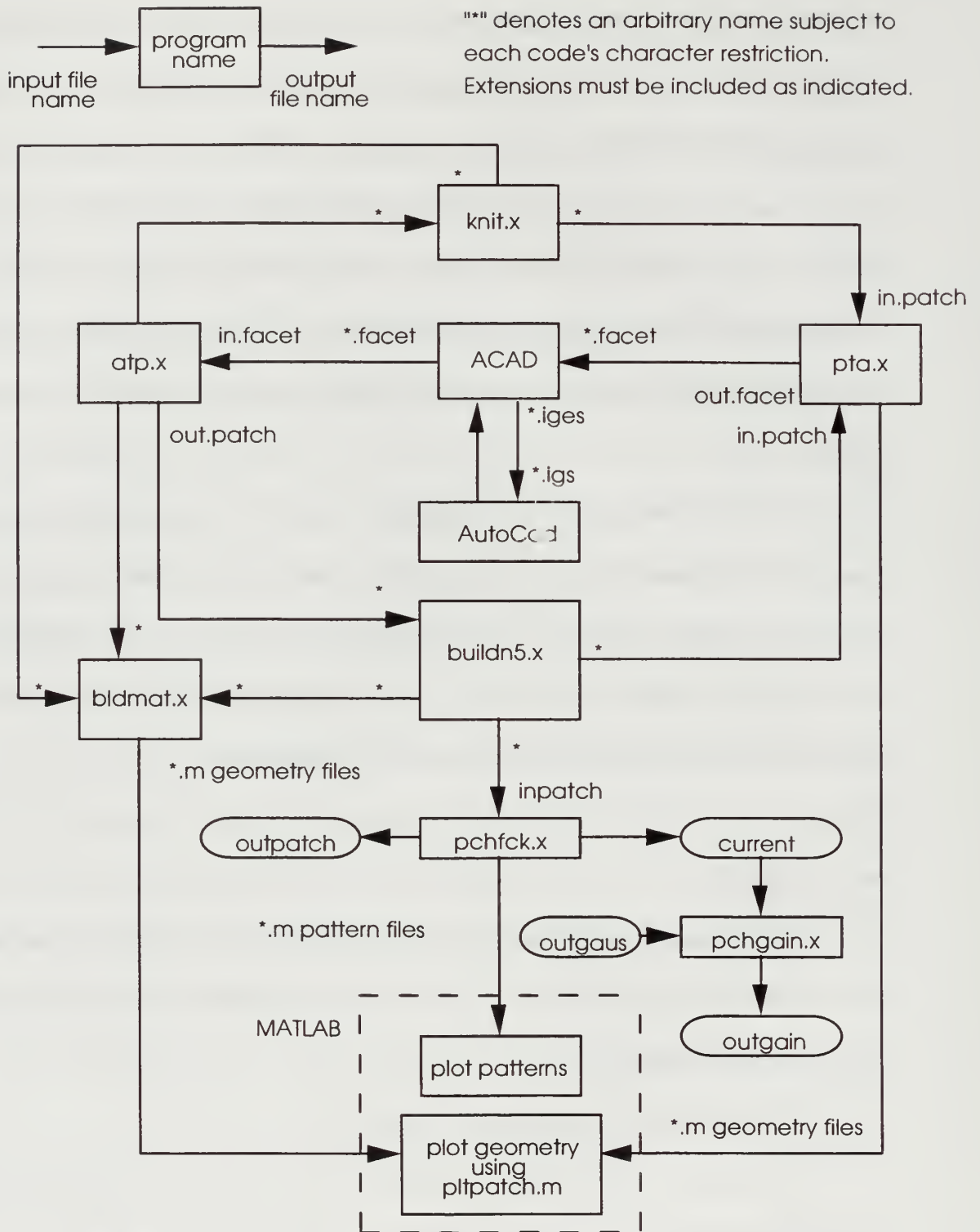
Figure 3.1 The relationship between the **PATCH** code and the MATLAB script files (after [Ref. 7]). (**pchfck.x** is a version of PATCH that has some modifications and enhancements incorporated.)

18

2.   Determine the nodes and the edges for voltage excitation.

Using **bldmat.x,** the output antenna model file from step 1 is converted to a format that can be plotted using the MATLAB script **pltpatch5.m.** **pltpatch5.m** provides the ability to view the antenna as well as label nodes, edges, and faces that are used to identify where the antenna is excited and where any lumped impedance is added. Also we can view the antenna in parts or in its entirety.

3.   Create the file **inpatch**.

Once the excitation edge number (i.e. the antenna feed point) is determined it is used along with the CAD file from step 1 to create an **inpatch** file. The code **pchfck.x** reads **inpatch** upon execution.

4.   Run **pchfck.x**.

The code **pchfck.x** is a modification of **patch.x**, which has some geometry checking procedures added to make sure that the nodes, edges, and faces provided are consistent and valid (the facet models considered for this problem are relatively small and therefore the CPU times are only several minutes). The code **pchfck.x** creates the following files: **outpatch, current, patchdat**, and the pattern M-files: **ampt.m, ampp.m, phi.m, theta.m**. We can view the pattern of the antenna in both horizontal and vertical planes using MATLAB. The file **outpatch** contains the current coefficients which can be used to compute the impedance. The file **current** is used by the code **pchgain.x** for computing the antenna gain.

5. Compute the gain.

The directivity and gain computation are done by numerically evaluating

$$D = \frac{4\pi}{\Omega_A} \qquad \text{(III-2)}$$

where

$$\Omega_A = \frac{1}{\left|\overline{E}_{max}\right|^2} \int_0^{2\pi}\int_0^{\pi} \left|\overline{E}(\theta,\phi)\right|^2 \sin(\theta)d\theta d\phi$$

and $\overline{E}_{max}$ is maximum electric field. A user must provide the file **outgaus**, which will be used by **pchgain.x** to compute the radiated power and the gain. **outgaus** contains integration constants for Gaussian quadrature numerical integration. The **pchgain.x** output is saved in an ASCII file named **outgain**.

C.   NEC-WIN

NEC-Win is user friendly because of its graphical user's interface. Each wire has a tag and can be divided into an arbitrary number of segments. The limit for the number of wires depends on the amount of computer memory. For example, with 8 MB of RAM, the Windows environment uses about 3 MB, and then **NEC-Win** can use as much as 5 MB of RAM. Therefore, the antenna model can have about 559 segments. This number is computed using the general rule [Ref. 8]

$$N_{MAX} = \sqrt{\frac{RAM}{16}} \qquad \text{(III-3)}$$

where N_{MAX} is the maximum number of segments, and RAM is the available memory. In general the segment lengths should not exceed 0.1 wavelength. For straight long

wires, longer segment lengths might be acceptable. The maximum wire radius is also dependent on wavelength, and it should follow the rule [Ref. 8]

$$\frac{(2\pi a)}{\lambda} << 1 \qquad \text{(III-4)}$$

where a is the wire radius, and λ is the wavelength.

IV. ANTENNA DESIGN AND SIMULATION

A. INTRODUCTION

Several candidate antenna configurations were simulated using **PATCH** and **NEC-Win**. They included a monopole on a disk, a top-loaded monopole, a monopole on a cylindrical cap, and a circular loop over a disk. All of the antennas contain a conducting disk, which represents the bottom surface of the MRPV body. The metallic disk serves three functions:

    1.   structural mount for the wire element,

    2.   provides some additional directivity by acting as a ground plane, and

    3.   provides shielding for internal electronic devices.

Before proceeding with the antenna design, the accuracy of the two codes is determined for the basic geometry of interest. The impedance results of both codes were compared to the results from published theoretical and measured data by Meier and Summers [Ref. 3]. In Ref. 3, the input impedance of a monopole with a circular disk is presented for

- $h = 0.224\lambda$

- $a = 0.003\lambda$

- $\rho = 1\lambda$

where h is the length of the monopole antenna, a is the radius of the monopole wire, λ is the wavelength, and ρ is the radius of the disk.

The chosen frequency for the antenna calculations is 1 GHz (λ=3 m). Therefore, the dimensions for the test case in meters are $h = 0.0672$ m, $a = 0.0009$ m, and $\rho = 0.3$

m. In **PATCH** the circular monopole wire is modeled as a thin strip of width w. The equivalent radius of a thin strip is $a_e=0.25w$ [Ref. 5] so that the equivalent width of a thin wire is

$$w_e = 4a. \qquad\qquad (\text{IV-1})$$

The test results are shown in Table 4.1. The results of **PATCH** are more accurate than those from **NEC-Win**, as expected. The imaginary part (reactance) of the input impedance converges more slowly than the real part (resistance). The **NEC-Win** data could probably be improved by adjusting the mesh density and wire radius. However, there is no reliable guideline for setting the parameters for the optimum results beforehand. This is a major disadvantage of the wire mesh model in general.

Table 4.1. Summary of input impedance validation test.

Methods	$R_{in} = \text{Re}\{Z_{in}\}$ [Ohm]	$X_{in} = \text{Im}\{Z_{in}\}$ [Ohm]
Theoretical	34.5	-8.0
Measured	34.0	-6.8
PATCH	31.9	-10.8
NEC-Win	34.0	-0.2

B.   COMPUTED RESULTS

The major challenge in designing the antenna is to adjust the parameters so that the reactive part of the input impedance is zero. Physically this component is due to the capacitance and inductance of the antenna configuration. The reactive part of the impedance can be a rapidly varying function of several of the geometrical parameters. It

is often necessary to look at many iterations of the geometry with very small changes to find the combination of dimensions that gives a real input impedance.

As described in Chapter I, the objective is to design an antenna that has an input impedance of 50 Ohms, that is, $Z_{in} = R_{in}+jX_{in} = 50+j0$ Ohms. This would yield a VSWR of 1. However, a VSWR of 2:1 is acceptable. Thus R_{in} could be in the range 25 Ohms $\leq R_{in} \leq$ 100 Ohms, if $X_{in}=0$. Ideally we would like to adjust the geometry so that the input resistance is 50 Ohms. This is not as important as eliminating the reactive part because a transformer section could be added to fine tune R_{in}.

Four antenna configurations were modeled in **PATCH** and **NEC-Win**. Three models are variations of the monopole antenna with a disk, and the fourth is a loop over a disk. The **PATCH** models are shown in Figures 4.1 through 4.4:

1. monopole with a disk (Figure 4.1),

2. top-loaded monopole with a disk (Figure 4.2),

3. monopole on a cylindrical cap (Figure 4.3), and
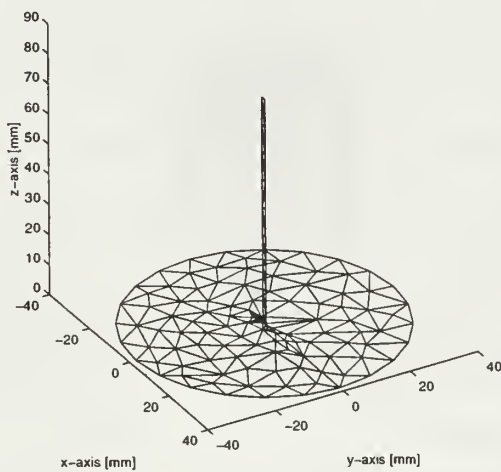
4. circular loop above a disk (Figure 4.4).

Figure 4.1 The **PATCH** model of the monopole antenna with a disk.

The top loading and the addition of the cylinder in 2 and 3 were attempts to tune out the reactive part of the impedance.
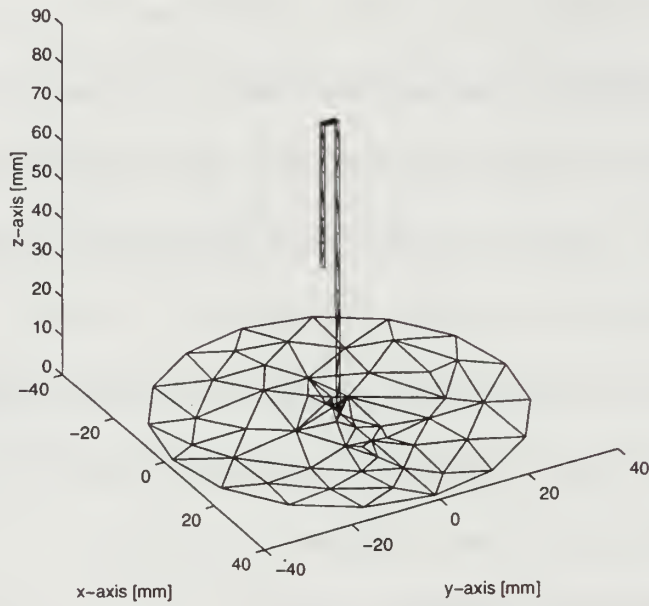

Figure 4.2 The **PATCH** model of the top-loaded monopole with a disk.
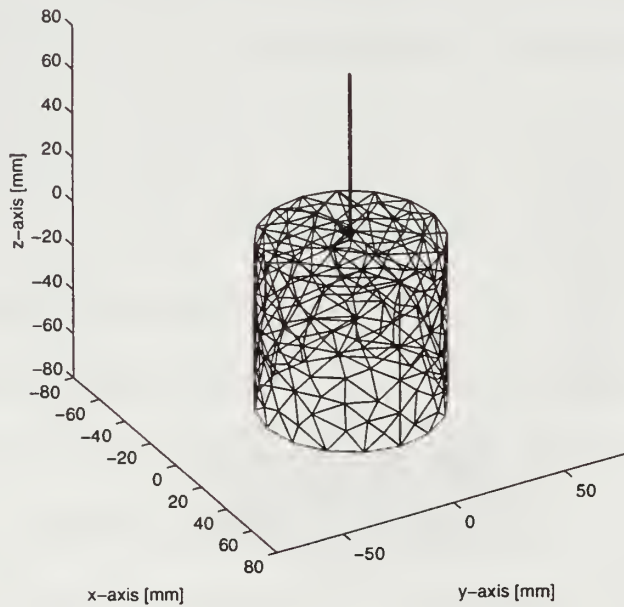
Figure 4.3 The **PATCH** model of the monopole antenna on a cylindrical body.
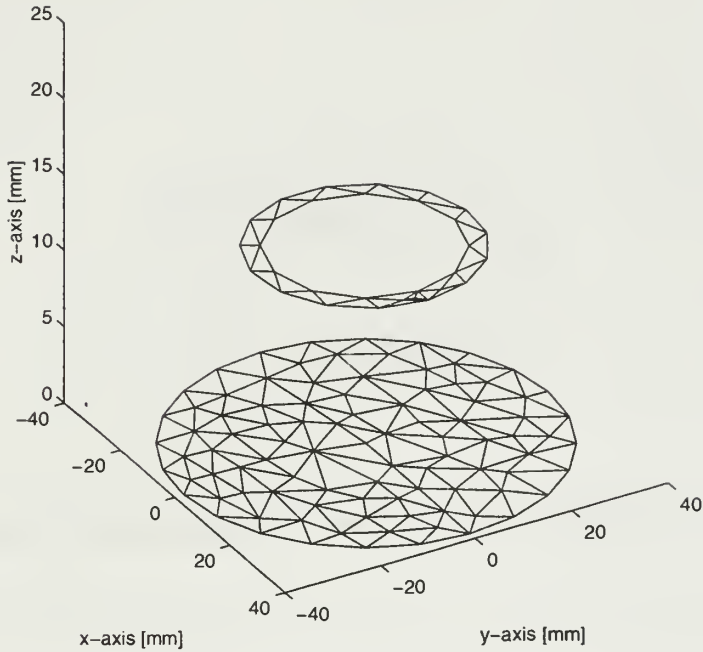
Figure 4.4 The **PATCH** model of the circular loop above a disk.

1.   NEC-Win simulation

The wire grid **NEC-Win** models are shown in Figures 4.5 through 4.8. The input

files for the results in Tables 4.2 through 4.5 can be found in Appendix A. Data is shown

for the calculation frequencies (f) of 1.0, 1.5 and 2.0 GHz. The columns R_{ADD} and X_{ADD}

are the series lumped resistance and reactance added across the input terminals. Since

NEC-Win does not have the capability to include lumped loads, these entries are zero.

NEC-Win determines the input impedance by simply dividing the impressed voltage at

the fixed point by the computed current. The data shows that the cylindrical end cap is

the most effective in reducing the reactive part of the input impedance.

Figure 4.5 The **NEC-Win** model of the monopole antenna with a disk.

Figure 4.6 The **NEC-Win** model of the top-loaded monopole with a disk.

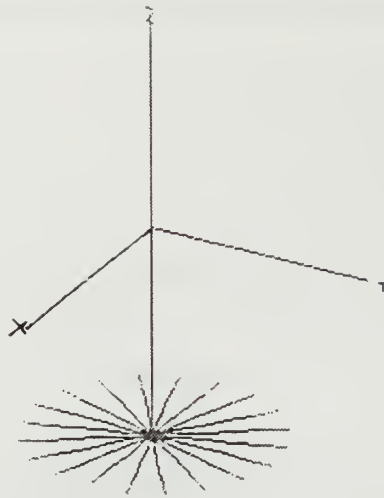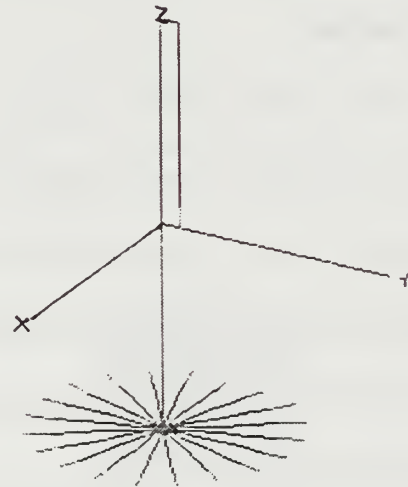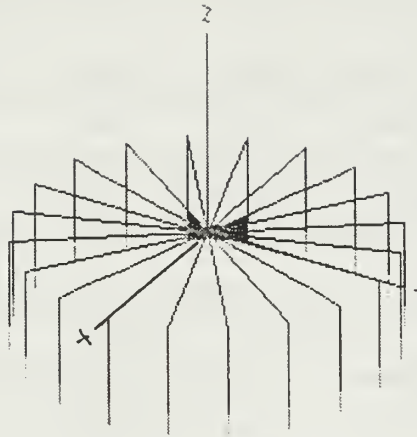Figure 4.7 The **NEC-Win** model of the monopole antenna on a cylindrical body.
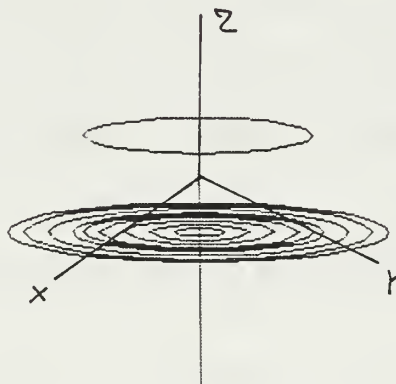
Figure 4.8 The **NEC-Win** model of the circular loop above a disk.

Table 4.2. **NEC-Win** results for a monopole antenna with a disk.

f [GHz]	R_{ADD} [Ohm]	X_{ADD} [Ohm]	R_L [Ohm]	X_L [Ohm]	Gain [dB]	VSWR
1.0	0.00	0.00	25	-60	1.90	7.0
1.5	0.00	0.00	123	140	1.80	6.2
2.0	0.00	0.00	435	-260	2.00	11.9

Table 4.3. **NEC-Win** results for a monopole top-loaded with a hook and a disk.

f [GHz]	R_{ADD} [Ohm]	X_{ADD} [Ohm]	R_L [Ohm]	X_L [Ohm]	Gain [dB]	VSWR
1.0	0.00	0.00	20	-30	2.1	3.0
1.5	0.00	0.00	520	430	2.0	17.5
2.0	0.00	0.00	110	25	2.0	1.7

Table 4.4. **NEC-Win** results for a monopole antenna with a cylindrical disk.

f [GHz]	R_{ADD} [Ohm]	X_{ADD} [Ohm]	R_L [Ohm]	X_L [Ohm]	Gain [dB]	VSWR
1.0	0.00	0.00	50	30	2.1	1.8
1.5	0.00	0.00	260	170	1.2	7.2
2.0	0.00	0.00	560	-275	1.3	13.6

Table 4.5. **NEC-Win** results for a circular loop antenna with a disk.

h [mm]	R_L [Ohm]	X_L [Ohm]
5	13.6	461
9	81.0	1390
13	257	2290
20	910	3620

2.   PATCH simulation

PATCH provides the ability to include lumped loads ($R_{ADD}+jX_{ADD}$). This is one possible way to get rid of the imaginary part of the input impedance. However, lumped elements are bulky and heavy, and it is more efficient to avoid using them. Top loading the monopole or adding the cylindrical walls to the disk are ways to affect the input impedance without using lumped elements. As in the case of **NEC-Win**, the **PATCH** results show that the cylindrical wall version has negligible reactance without adding a lumped load.

Table 4.6. **PATCH** results for a monopole antenna with a disk.

f [GHz]	R_{ADD} [Ohm]	X_{ADD} [Ohm]	R_L [Ohm]	X_L [Ohm]	Gain [dB]	VSWR
1.0	0.00	0.00	20.600	-11.720	1.73050	2.60
1.0	29.40	11.72	50.010	0.004	1.73050	1.00

Table 4.7. **PATCH** results for a monopole antenna top-loaded with a hook and a disk.

f [GHz]	R_{ADD} [Ohm]	X_{ADD} [Ohm]	R_L [Ohm]	X_L [Ohm]	Gain [dB]	VSWR
1.0	0.00	0.00	36.13	113.25	1.76419	9.80
1.0	13.87	-113.25	50.00	0.0019	1.76420	1.01

Table 4.8. **PATCH** results for a monopole antenna with a cylindrical body.

f [GHz]	R_{ADD} [Ohm]	X_{ADD} [Ohm]	R_L [Ohm]	X_L [Ohm]	Gain [dB]	VSWR
1.0	0.00	0.00	49.840	-4.297	2.39100	1.08
1.01	0.00	0.00	50.610	-0.486	2.42409	1.10
1.0113	0.00	0.00	50.700	0.008	2.42840	1.02

Table 4.9. **PATCH** results for a circular loop antenna with a disk.

h [mm]	R_L [Ohm]	X_L [Ohm]
5	10.5	1797
9	43.0	2467
13	100.7	2971
20	232.0	3529

The calculation of impedance for the **PATCH** model is explained with the use of Figure 4.9. The feed is represented as an edge in the **PATCH** model. The surface current is

$$\bar{J}_s = J_s \hat{z} \qquad \text{(IV-2)}$$

where $\hat{z}$ is a unit vector parallel to the strip and J_s is a complex quantity obtained from the file **outpatch**. Since the strip is thin and the excited edge is perpendicular to the z axis, the total current crossing the edge is

$$I = J_s \hat{z} \cdot \hat{z} w = J_s w. \qquad \text{(IV-3)}$$

The impedance is obtained by dividing the impressed voltage by I.

From the results in Tables 4.6 through 4.9, the best design choice is the one with a cylindrical body because it does not need an external lumped impedance. This conclusion is consistent with the **NEC-Win** data as well.
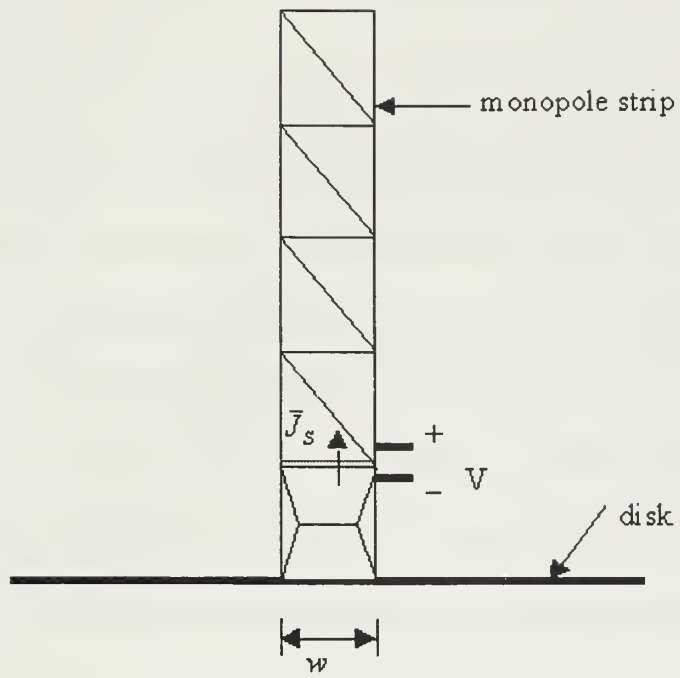
Figure 4.9 Partial view of the **PATCH** model.

V. SUMMARY AND FUTURE WORK

The objective of this research was to design a compact lightweight communications antenna for a MRPV. The antenna will be used to transmit and receive video and telemetry data between the MRPV and the ground station. Therefore the pattern must be hemispherical (constant gain in the lower hemisphere). Dipoles, monopoles, and loops are suitable antennas, even though there will be a notch in the gain directivity below the vehicle. Under most conditions, the MRPV will be at low altitude far from the ground station and, therefore, the *zenith* angle θ is approximately 90°. Fortunately this is the direction of the maximum gain for all of the above mentioned antenna types.

Based on a computer simulation of four antenna configurations, it is recommended that a monopole on a cylindrical end cap be selected as the design. This configuration had the lowest VSWR at 1.0113 GHz (1.02:1) and an input impedance of Z_{in} = 50.7+j0.008 Ohms. The VSWR is slightly higher at 1.0 GHz but still has a value well below the design goal.

The frequency of 1 GHz is at the high end of the range of frequencies typically used for a video and telemetry. A frequency as low as 100 MHz could be used, but the hardware (transmitter and receiver) is larger and heavier than at the higher frequencies. If necessary, the antenna dimensions could be frequency scaled. Some additional fine-tuning would probably be required.

Antennas for future MRPV designs could be integrated into the body as in the case of the microwave powered version. New MRPV concepts incorporate a rotor guard

which could be used as a foundation for a loop. Also, there will be three or four short leg

wires for landing. One or several of these could possibly be used as antenna.

APPENDIX A.   EXAMPLES OF NEC-WIN INPUT FILES

This appendix contains listings of all **NEC-Win** input files that were used to get the results posted in Chapter IV. These **NEC-Win** files are:

1.   **Test.nec**,

2.   **Disk.nec**,

3.   **TopLoad.nec**,

4.   **Body.nec**, and

5.   **Ring.nec**.

Test.nec is designed to simulate the monopole antenna (length of 67.2 mm and radius of 0.9 mm) with a disk diameter of 300 mm. The calculation frequencies are 0.9, 1.0, and 1.1 GHz.

Disk.nec is designed to simulate the monopole antenna (length of 75 mm and radius of 0.9 mm) with a disk diameter of 38.1 mm. The calculation frequencies are 1.0, 1.5, and 2.0 GHz.

TopLoad.nec is designed to simulate the monopole antenna (length of 75 mm and radius of 0.9 mm) with a disk diameter of 38.1 mm and a hook length of 37.5 mm. The calculation frequencies are 1.0, 1.5, and 2.0 GHz.

Body.nec is designed to simulate the monopole antenna (length of 75 mm and radius of 0.9 mm) with a cylindrical body diameter of 38.1 mm and height of 75 mm. The calculation frequencies are 1.0, 1.5, and 2.0 GHz.

Ring.nec is designed to simulate the circular loop antenna (radius of 22.8 mm) over a disk of radius of 38.1 mm. The calculation frequencies are 1.0, 1.5, and 2.0 GHz.

Program 1   Test.nec

CM NEC-WIN
CM Simple monopole antenna in Free Space with a disc
CM With a disc radius 0.3 m
CM Pole Length 0.0672 m with radius 0.0009 m
CM Operated at frequency 0.9, 1.0, 1.1 GHz
CE
GW 2,10, 0,0,0, 0,.3,0, .0009
GR 1 20
GW 1,10, 0,0,0, 0,0,.0672, .0009
GS 0 0 1
GE 0
GN -1
EX 0 1 1 11 1 0
FR 0 3 0 0 900 100
RP 0 361 1 1000 0 0 1 1
RP 0 1 361 1000 0 0 1 1
EN

Program 2   Disk.nec

CM NEC-WIN
CM Monopole antenna in Free Space with a finite disc
CM With a disc radius 0.01905 m
CM Pole Length 0.075 m
CM Operation Frequency from 900 MHz to 1250 MHz
CE
GW 2,5, 0,0,0, 0,.01905,0, .0009
GR 1 20
GW 1,10, 0,0,0, 0,0,.075, .0009
GS 0 0 1
GE 0
GN -1
EX 0 1 1 11 1 0
FR 0 3 0 0 1000 500
RP 0 361 1 1000 0 0 1 1
RP 0 1 361 1000 0 0 1 1
EN

Program 3   TopLoad.nec

```
CM NEC-WIN
CM Monopole antenna in Free Space with hook and disc
CM With a disc radius 0.01905 m
CM Pole Length 0.075 m with radius 0.0009 m
CM Hook length 0.0375 m with radius 0.0009 m
CM Operation Frequency from 900 MHz to 1250 MHz
CE
GW 4,5, 0,0,0, 0,0.01905,0, .0009
GR 1 20
GW 1,10, 0,0,0, 0,0,.075, .0009
GW 2,1, 0,0,0.075, 0.0005,0,0.075, 0.0009
GW 3,5, 0.0005,0,0.075, 0.0005,0,0.0375, .0009
GS 0 0 1
GE 0
GN -1
EX 0 1 1 11 1 0
FR 0 3 0 0 1000 500
RP 0 361 1 1000 0 0 1 1
RP 0 1 361 1000 0 0 1 1
EN
```

Program 4   Body.nec

```
CM NEC-WIN
CM Monopole antenna in Free Space with cylinder body
CM Pole Length 0.075 m with radius 0.0009 m
CM Cylinder body high 0.075 m radius 0.01905 m
CM Operation Frequency from 900 MHz to 1250 MHz
CE
GW 2,5, 0,.12,0, 0,.12,-.075, .0009
GW 3,5, 0,0,0, 0,0.12,0, 0.0009
GR 1 20
GW 1,9, 0,0,0, 0,0,.075, .0009
GS 0 0 1
GE 0
GN -1
EX 0 1 1 11 1 0
FR 0 3 0 0 1000 500
RP 0 361 1 1000 0 0 1 1
RP 0 1 361 1000 0 0 1 1
EN
```

Program 5 Ring.nec

```
CM NEC-WIN
CM The Ring antenna in Free Space
CM With a disc radius 0.01905 m
CM width 0.00375 m hight = 0.020 m ring radius 0.0228
CM Operation Frequency from 900 MHz to 1250 MHz
CE
GA 2 30 0.0381 0 360 0.0009375
GA 3 30 0.03 0 360 0.0009375
GA 4 20 0.025 0 360 0.0009375
GA 5 10 0.02 0 360 0.0009375
GA 6 10 0.015 0 360 0.0009375
GA 7 10 0.01 0 360 0.0009375
GA 8 10 0.005 0 360 0.0009375
GA 9 20 0.035 0 360 0.0009375
GA 10 20 0.0228 0 360 0.0009375
GM 1 0 0 0 0 0 0 0.020 0 0
GA 1 20 0.0228 0 359 0.0009375
GS 0 0 1
GE 0
GN -1
EX 0 1 20 00  1.00000  0.00000
FR 0 6 0 0 998 1
RP 0 361 1 1000 0 0 1 1
RP 0 1 361 1000 0 0 1 1
EN
```

40

LIST OF REFERENCES

[1] David C. Jenn, "Tiny, microwave powered, remotely piloted vehicles," *IEEE Potentials*, Vol. 16, No. 5, pp.20-22, Dec. 97.

[2] First International Conference on Emerging Technologies for Micro UAVs, Georgia Tech., Feb. 1997.

[3] Warren L. Stutzman and Gary A. Thiele, *Antenna Theory and Design*, John Wiley & Sons, Inc., New York, 1981.

[4] Robert E. Collin, *Antennas and Radiowave Propagation*, McGraw-Hill, New York, 1985.

[5] John D. Kraus, *Electromagnetics*, McGraw-Hill Inc., New York, 1992.

[6] David C. Jenn, *Radar and Laser Cross Section Engineering*, The American Institute of Aeronautics and Astronautics, Washington DC, 1995.

[7] W.A. Johnson, *PATCH Code User's Manual*, Sandia Labs Report SAND87-2991, May, 1988.

[8] *NEC-Win Pro User's Manual*, Nittany Scientific, Inc., Hollister, CA, Feb. 1997.

INITIAL DISTRIBUTION LIST

No. Copies

1. Defense Technical Information Center 2
   8725 John J. Kingman Rd., ste 0944
   Ft. Belvoir, Virginia 22060-6218

2. Dudley Knox Library 2
   Naval Postgraduate School
   411 Dyer Rd.
   Monterey, California 93943-5101

3. Prof. David C. Jenn, Code EC/Jn 2
   Department of Electrical and Computer Engineering
   Monterey, California 93943-5121

4. Dr. Supachai Sirayanone, Code MR/SY 1
   Department of Meteorology
   Monterey, California 93943-5121

5. Prof. Dan C. Boger, Code CS/Bo 1
   Department of Computer Science
   Monterey, California 93943-5121

6. CDR. Michael T. McMaster, Code 37 1
   Undersea, Space and Information Warfare
   Monterey, California 93943-5121

7. Office of the Air Attaché, Royal Thai Embassy 3
   1024 Wisconsin Ave., N.W., Suite 303
   Washington, DC 20007

8. Pimada Chusakulvanich 1
   3416 W. Orange Ave., Apt # 218
   Anaheim, California 92804

9. Lt. Piya Limsakul 1
   Naval Postgraduate School
   2 University circle, SGC 1389
   Monterey, California 93943

10. 2Lt. Narongdech Suksong 1
    59/285 Homeplace Village, soi 18
    Ramkhumhang road, Sapansoong
    Beungkum, Bangkok 10240
    THAILAND